ChemComm

Single crystalline tantalum oxychloride microcubes: controllable synthesis, formation mechanism and enhanced photocatalytic hydrogen production activity

Journal:	*ChemComm*
Manuscript ID:	CC-COM-04-2015-003455.R1
Article Type:	Communication
Date Submitted by the Author:	23-Jun-2015
Complete List of Authors:	Tu, Hao; Wuhan University of Technology, Xu, Leilei; Wuhan University of Technology, State Key Laboratory of Advanced Technology for Materials Synthesis and Processing, Wuhan University of Technology Guan, Jianguo; Wuhan University of Technology, Mou, Fangzhi; Wuhan University of Technology,

Journal Name

COMMUNICATION

Single crystalline tantalum oxychloride microcubes: controllable synthesis, formation mechanism and enhanced photocatalytic hydrogen production activity

Received 00th January 20xx,
Accepted 00th January 20xx

DOI: 10.1039/x0xx00000x

www.rsc.org/

Hao Tu,[a,b] Leilei Xu,[a,b] Fangzhi Mou,[a] and Jianguo Guan*,[a]

Single crystalline microcubes of a new tantalum compound, tantalum oxychloride ($TaO_{2.18}Cl_{0.64}$), have been fabricated hydrothermally in a concentrated aqueous solution of hydrochloric acid and acetic acid. They contain a superstructure and exhibit remarkably enhanced photocatalytic activities for hydrogen production due to the improved light harvest and facilitated charge transport.

Single crystalline micro- or nanoparticles exhibit facilitated charge transport and increased long-range electronic connectivity,[1] and thus have remarkable applications in high performance gas sensing,[2] antibacterial,[3] or photocatalysis[4] due to the low defect density and less grain boundaries. In addition, their crystallographic orientation, exposed facets or surface structures also show strong influences on the free energy as well as the electronic, optical and magnetic performances. This makes it attractive to fabricate the nano or micro single crystals in various shapes or specific exposed facets,[5] such as TiO_2,[6] Co_3O_4,[5a] Ag_2O[3] and so on.

Tantalum oxides, as an important class of semiconductors, have been widely applied in dielectric,[7] coating,[8] and photocatalytic fields.[9] However, most tantalum oxides obtained so far only exhibit amorphous and polycrystalline characters due to the extremely rapid hydrolysis of Ta^{5+} ions in most solutions as well as the chemical inertness of the corresponding hydrolysates.[10] Recently, one dimensional (1D) Ta_2O_5 nanowires or hierarchical nanostructures (HNSs) composed of single crystalline Ta_2O_5 nanorods have been fabricated by in-situ hydrolyzing the intermediate H_2TaF_7 generated slowly via etching Ta powders with hydrofluoric acid (HF) and hydrogen peroxide under a hydrothermal condition.[9,11] In such a process, the strongly corrosive HF is a requisite, which unavoidably results in defects to induce secondary nucleation of tantalum oxides. Additionally, the as-obtained 1D nanostructures or HNSs of tantalum oxides both expose the same facets, hampering the decipherment of the relationship between the chemophysical properties and the exposed facets. Nevertheless, direct hydrolysis of Ta^{5+} ions into single crystalline particles, especially with the exposed facets different from those of the aforementioned 1D nanostructures or HNSs in a non-fluorine environment is still a great challenge.

In this communication, we have for the first time prepared single crystalline tantalum oxychloride microcubes ($TaO_{2.18}Cl_{0.64}$ MCs) with a superstructure by controlling the hydrolysis of tantalum chloride in a concentrated solution of hydrochloric acid (HCl) and acetic acid (HAc) under hydrothermal conditions. In this protocol, HAc, as a buffer, is able to elaborately regulate the growth kinetics of the single crystalline $TaO_{2.18}Cl_{0.64}$ MCs via keeping the solution acidity stable. Being free of grain boundary and impurity, as well as the introduction of halide ions into the crystal lattice, the as-obtained single crystalline $TaO_{2.18}Cl_{0.64}$ MCs exhibit an attractively enhanced photocatalytic activity for hydrogen production, which is far more than those of the HNSs of single crystalline Ta_2O_5 nanorods and commercial Ta_2O_5, owing to the accelerated charge transfer[12] and improved light harvest.[13]

In a typical synthesis, 60 mg of $TaCl_5$ powers were dissolved in 30 mL of 4 M HCl and 12 M HAc aqueous solution, and then solvothermally treated at 200 °C for 10 h. The as-prepared samples are microcubes with edge lengths of about 1.5 - 2 μm (Fig. 1a), and have a single-crystalline nature (Fig. 1b). They are composed of Ta, O and Cl elements (Fig. S1a), which uniformly distribute in the bulk (Fig. S2). Among them, the element Ta exists in a form of Ta^{5+} (Fig. S1b), [9,14] while Cl exists in both the surface and the lattices, and the valences of Cl and O are -1 and -2, respectively (Fig. S1c and d). Combining the valences of Ta, O and Cl atoms and the XRF result (see the chemical composition characterization, ESI), the element ratio of Ta : O : Cl in the as-obtained samples is estimated to be 1 : 2.18 : 0.64, and thus they can be formulated as $TaO_{2.18}Cl_{0.64}$.

[a] State Key Laboratory of Advanced Technology for Materials Synthesis and Processing, Wuhan University of Technology, 122 Luoshi Road, Wuhan, 430070, P. R. China.
[b] These two authors contributed equally to the work.
* Corresponding author. E-mail: guanjg@whut.edu.cn; Fax: 86-27-87879468; Tel:89-27-87218832.
Electronic Supplementary Information (ESI) available: [Details of Synthesis of $TaO_{2.18}Cl_{0.64}$ MCs, Characterization of $TaO_{2.18}Cl_{0.64}$ MCs, Photocatalytic Tests, Electrochemical measurement, Structure simulation; Table. S1; Fig. S1 to S15. See DOI: 10.1039/x0xx00000x

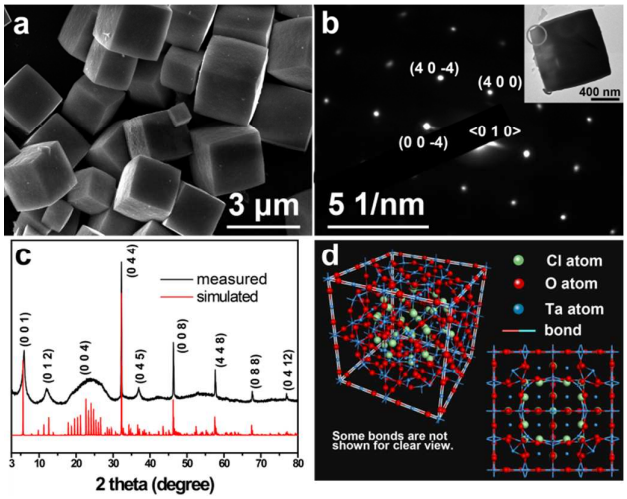

Fig. 1 SEM image (a), SAED (b), XRD patterns (c) and the superstructure schematic (d) of the as-obtained $TaO_{2.18}Cl_{0.64}$ MCs. The circled area in the inset of (b) shows where the SAED comes from.

Fig. 1c shows the measured XRD pattern of the $TaO_{2.18}Cl_{0.64}$ samples. Obviously, it is entirely different from the standard pattern of (PDF#89-2843), but its peaks at 32.3°, 46.3°, 57.7°, 67.6° and 76.8° are almost consistent with the diffraction spectra of BaTe (PDF#65-7592) and TaO_2F (PDF#76-2370), except the three unusual broadened peaks below 30° (in Fig. S3a). This suggests that the as-obtained $TaO_{2.18}Cl_{0.64}$ microcubes are not doped Ta_2O_5 by Cl^{-1} ions, but have the similar crystalline structure to BaTe and TaO_2F.[15] The difference between the measured pattern and the one of standard TaO_2F may be ascribed to the partial lack of the body-center atoms in $TaO_{2.18}Cl_{0.64}$ lattice. The three unusual broadened peaks below 30° indicate the regional disorder of the crystal lattice and superstructure, resulted from the partial substitution of Cl atoms with a much large diameter for O atoms, as the bond length of X-Ta (X means anions) changes with the X species in the tantalum oxyhalide.[16] In other words, the arched peak at about 23° corresponds to the disordered Ta atoms at the body-center sites, caused by the significantly differentiated bond length between Ta-O and Ta-Cl. The broadened peaks around 2.5° to 15° indicate that the $TaO_{2.18}Cl_{0.64}$ MCs have a superstructure with a long range symmetry. Fig. 1d illustrates the superstructure features of the $TaO_{2.18}Cl_{0.64}$ microcubes with some distortions in a size of about 4 × 4 cells (more explanation in ESI). Using this model with the details in Table S1, we are able to obtain the simulated XRD pattern (the red line in Fig. 1c), which is almost identical to the measured one (black line). This suggests that the as-obtained microcubes possess the crystalline lattices shown in Fig. 1d. Fig. S3b indicates that after the typical $TaO_{2.18}Cl_{0.64}$ MCs are placed in the liquid nitrogen (below 77 K) for 36 h, the XRD diffraction peaks below 10° become strong. This further validates the superstructure of the as-prepared $TaO_{2.18}Cl_{0.64}$ MCs, as the long range symmetry of the superstructure could be improved if the thermal vibration is suppressed at a low temperature.[17]

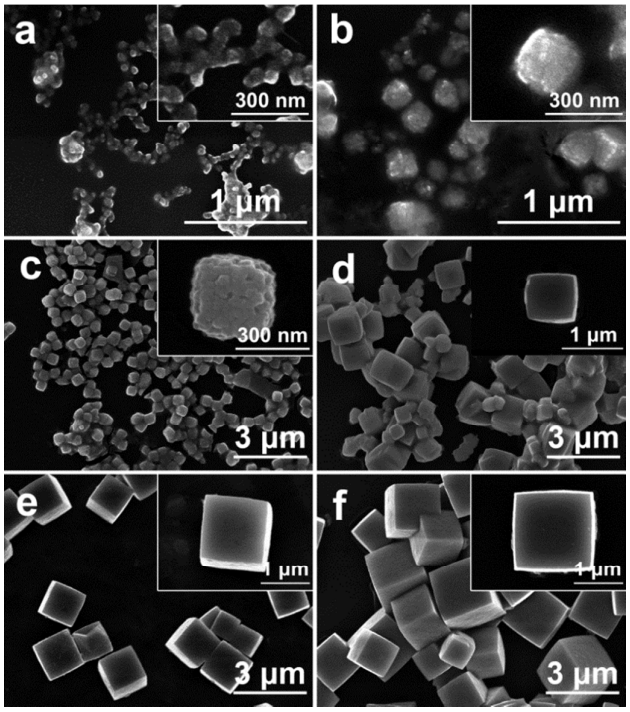

Fig. 2 SEM images of $TaO_{2.18}Cl_{0.64}$ MCs obtained at different solvothermal time (*t*). 35 min (a), 40 min (b), 1 h (c), 3 h (d), 8 h (e) and 12 h (f).

To elucidate the growth mechanism of $TaO_{2.18}Cl_{0.64}$ MCs, the influences of solvothermal time (*t*) on the structures and morphologies of the products have been investigated. Figs. 2a and b reveal that the aggregation of nanoparticles at about 40 min results in the MCs, which are composed of Ta, O and Cl elements, and some Cl^{-1} ions are incorporated into the crystal lattice evidenced by XPS (Fig. S4). With *t* increasing to 1 h, the nanoparticle aggregates grow into cube-like structure with discernible crystal boundaries and a size of 300 nm. As indicated by Fig. S5, the nanoparticles in the cube-like product are oriented attachment.[18] Further increasing *t* gradually increases the cube size. At the same time, the crystal boundaries between nanoparticles fade away and the cube surfaces become smooth. Consequently, the $TaO_{2.18}Cl_{0.64}$ MCs are obtained.

Fig. S6 indicates that all the samples obtained at different time have the same crystalline phase but with different crystallinities. In our protocol, $TaO_{2.18}Cl_{0.64}$ microcubes are generated via the following chemical reaction equations[19,20]:

$$Ta^{5+} + xCl^{-} + \frac{5-x}{2}H_2O \leftrightarrow TaO_{\frac{5-x}{2}}Cl_x + (5-x)H^{+} \quad (1)$$

$$CH_3COOH \leftrightarrow CH_3COO^{-} + H^{+} \quad (2)$$

As demonstrated in eqn. (1), the hydrolysis of Ta^{5+} is an equilibrium reaction, in which the net generation rate of $TaO_{2.18}Cl_{0.64}$ is related to both the positive and reverse reactions depending on the H^+ concentration ($[H^+]$) in the solution, which is determined by the dissociation of HCl and HAc. In the strong acidic environment of 4 M of HCl and 12 M of HAc, the hydrolysis equilibrium slightly shifts to the left.

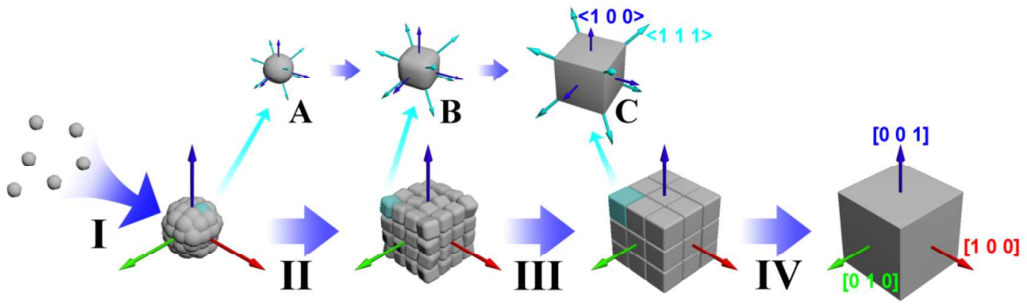

Scheme 1 Schematic diagram to Illustrate the formation mechanism of the $TaO_{2.18}Cl_{0.64}$ MCs. I. The oriented aggregation of the $TaO_{2.18}Cl_{0.64}$ nuclei formed by the hydrolysis of Ta^{5+}; II. Facets-selective crystal growth occurs with $R_{<100>}/R_{<111>}$ of 0.58 as $[H^+]$ is well regulated with an almost constant value, resulting in the formation of subunit nanocubes; III. The structural unit nanocubes further grow to make the crystal boundaries between the structural units merge together; IV. Further Crystal growth to obtain perfect single crystalline $TaO_{2.18}Cl_{0.64}$ MCs. A, B and C are the magnification of the corresponding structural units, respectively.

Consequently, the net reaction rate of eqn (1) is slow enough to match with the nucleation and growth rates of the $TaO_{2.18}Cl_{0.64}$ product so that the anisotropic growth of the $TaO_{2.18}Cl_{0.64}$ product occurs with selective crystallographic facets. Since HAc is a weak acid and its dissociation equilibrium is closely related to $[H^+]$. With the hydrolysis reaction of Ta^{5+} proceeding, $[H^+]$ increases. In this case, the dissociation of HAc is restrained to ensure the acidity of solution stable (eqn. 2). Simultaneously, the product can be formed at an extremely low and steady rate in the entire hydrolysis process. The detailed formation mechanism of the as-prepared $TaO_{2.18}Cl_{0.64}$ MCs is described in Scheme 1. At the beginning, the freshly formed nanoparticles aggregate in an oriented attachment manner to decrease the surface energy. Since the elaborately adopted concentrated acidic environment can create a quasi-equilibrium growth environment, in which, for example, the ratio of growth rate along <100> into that along <111> is about 0.58,[21, 22] producing a cubic structural unit with exposing {100} due to its lowest surface free energy. [23] As the reaction time goes on, the crystal boundaries between the cubic structural units are preferentially filled with the generated atoms because of its high surface energy. After further crystal growth, the final $TaO_{2.18}Cl_{0.64}$ MCs are obtained.

The above proposed formation mechanism of the as-prepared $TaO_{2.18}Cl_{0.64}$ MCs has been further approved by the little influences of the Ta source species on the formation of the MCs (Fig. S7). Figs. S8 and 9 indicate that the quasi-equilibrium reaction conditions of eqn (1) are mainly determined by [HCl], and would be destroyed with decreasing [HCl], resulting in the formation of irregular particles and/or aggregates with an amorphous phase. In addition to well-defined $[H^+]$ for initiating the eqn (1), HAc, as a buffer, has also an important contribution to make $[H^+]$ almost unchangeable in the whole reaction process. Fig. S10 evidences that there are both irregular particles and MCs in the resultant products at [HAc] = 8 M because the buffering capability of HAc is weak with decreasing [HAc]. Further decreasing [HAc] only produces irregular amorphous particles due to the reducing $[H^+]$ in the solution. This clearly confirms the dual contributions to the formation of the $TaO_{2.18}Cl_{0.64}$ MCs. In this regard, HAc can be replaced with other organic acids, such as propionic acid. Fig. S11 reveals that the MCs with an increased size can be obtained when HAc is substituted for propionic acid. This can be attributed to the weaker acidity of propionic acid than HAc, which will slightly increase the reaction extent of eqn (1), and thus enhances the conversion and size of the MCs. Fig. S12 shows the samples obtained at different solvothermal temperatures are all MCs, but show different particle sizes and crystallinities. This reveals that the solvothermal temperature mainly influences the quantity of the nucleus and the growth kinetics.

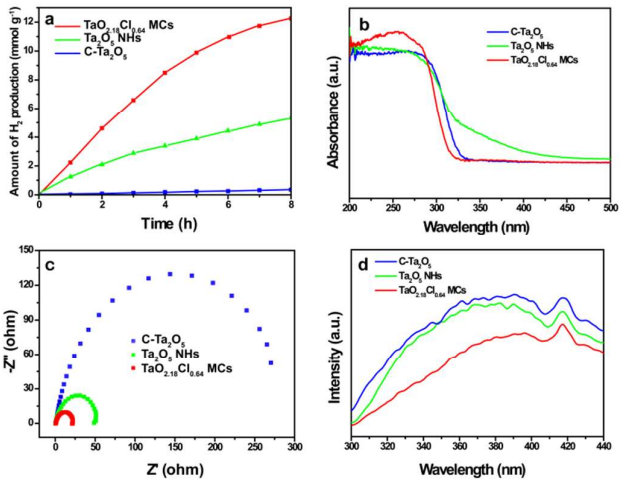

Fig. 3 (a) The photocatalytic activities for H_2 production after loading 5 wt% Pt in 30 vol% lactic acid aqueous solution, (b) UV-DR spectra, (c) EIS Nyquist plots and (d) PL spectra of the as-prepared $TaO_{2.18}Cl_{0.64}$ MCs, Ta_2O_5 HNs[9] and C-Ta_2O_5.

Fig. 3a shows that under simulant solar light irradiation for 8 h, the as-prepared $TaO_{2.18}Cl_{0.64}$ MCs in a 30 vol% lactic acid aqueous solution can produce above 12 mmol g^{-1} of H_2, much higher than that of the Ta_2O_5 NHs[9] and commercial Ta_2O_5 (C-Ta_2O_5). To exclude the effect of surface area, the specific surface H_2 evolution rate of the as-prepared $TaO_{2.18}Cl_{0.64}$ MCs was also calculated by averaging the specific surface area (Fig. S13). It reaches as high as 2473 μmol h^{-1} m^{-2}, 25 times bigger than the corresponding values of both C-Ta_2O_5 and Ta_2O_5 NHs,

further manifesting the significantly enhanced photocatalytic activity of the as-prepared $TaO_{2.18}Cl_{0.64}$ MCs. This, on one hand, can be attributed to the incorporation of Cl^- anions into the crystallographic lattice as well as the unique single crystalline structure. Due to the incorporation of Cl^- anions into the crystallographic lattice, Fig. 3b evidences that the as-prepared $TaO_{2.18}Cl_{0.64}$ MCs can more strongly absorb the light with wavelength below 280 nm than C-Ta_2O_5 and Ta_2O_5 HNs, and Fig. S14 further reveals that they have a more negative X-intercept of the linear region in the Mott-Schottky plots than C-Ta_2O_5, implying a much stronger reduction ability for the electrons transferred to its conduction band. Fig. 3c shows that the $TaO_{2.18}Cl_{0.64}$ MCs have a much smaller semicircle than C-Ta_2O_5 and Ta_2O_5 HNs in the EIS Nyquist plots,[12a] suggesting that the unique single crystalline structure endows them with an excellent conductivity of charge carriers. This favors the transfer of charge carriers.[12b] On the other hand, the superstructure of the $TaO_{2.18}Cl_{0.64}$ MCs can also contribute to the excellent charge transfer ability due to the existence of O vacancies induced by the large amount of chlorine anions in the lattice. This is approved by the lowest photoluminescence intensity of the as-prepared $TaO_{2.18}Cl_{0.64}$ MCs among the three samples (Fig. 3d). The as-prepared $TaO_{2.18}Cl_{0.64}$ MCs exhibits an excellent recyclability (Fig. S15) for H_2 production in 30 vol% lactic acid aqueous solution in the presence of Cl ions.

Conclusions

In conclusion, single crystalline $TaO_{2.18}Cl_{0.64}$ MCs have been prepared via a controllable hydrolysis of tantalum chloride in HCl-acetic acid aqueous solution. In this protocol, the well-defined almost constant strong acidic environment ensures a quasi-equilibrium condition for the whole hydrolysis reaction process of Ta^{5+} ions so that the anisotropic growth of the $TaO_{2.18}Cl_{0.64}$ product occurs with selective crystallographic facets. This is a new approach to obtain well crystalline Ta based oxides with a unique morphology. Strong acid-weak acid mixed solutions, such as the HCl-HAc system, are promising for the preparation of metal oxide single crystalline micro/nano-materials from the corresponding precursors with extremely rapid hydrolysis rates. The as-obtained $TaO_{2.18}Cl_{0.64}$ MCs are a new substance with superstructures containing disorders in the lattices. They show an enhancement in photocatalytic activity for hydrogen production due to the excellent charge transfer property, which stems from the unique monocrystalline structure with a special chemical composition.

Acknowledgement

This work was financially supported by the National Natural Science Foundation of China (51002111), the Natural Science Foundation of Hubei Province (2014CFB163 and 2015CFA003), the Top Talents Lead Cultivation Project of Hubei Province and the Fundamental Research Funds for the Central Universities (WUT: 2014-IV-131). We also thank M. Z. Lu, F. Wang for their discussion.

Notes and references

1. Y. C. Cho, S. Lee, M. Ajmal, W. K. Kim, C. R. Cho, S. Y. Jeong, J. H. Park, S. E. Park, S. Park, H. K. Pak and H. C. Kim, *Cryst. Growth Des.*, 2010, **10**, 2780-2784.
2. X. Wang, X. Han, S. Xie, Q. Kuang, Y. Jiang, S. Zhang, X. Mu, G. Chen, Z. Xie and L. Zheng, *Chem. Eur. J.*, 2012, **18**, 2283-2289.
3. X. Wang, H. F. Wu, Q. Kuang, R. B. Huang, Z. X. Xie and L. S. Zheng, *Langmuir*, 2009, **26**, 2774-2778.
4. (a) M. Liu, L. Piao, L. Zhao, S. Ju, Z. Yan, T. He, C. Zhou and W. Wang, *Chem. Commun.*, 2010, **46**, 1664-1666; (b) D. Q. Zhang, G. S. Li, X. F. Yang and J. C. Yu, *Chem. Commun.*, 2009, 4381-4383.
5. (a) X. L. Xiao, X. F. Liu, H. Zhao, D. F. Chen, F. Z. Liu, J. H. Xiang, Z. B. Hu and Y. D. Li, *Adv. Mater.*, 2012, **24**, 5762-5766; (b) X. G. Peng, L. Manna, W. D. Yang, J. Wickham, E. Scher, A. Kadavanich and A. P. Alivisatos, *Nature*, 2000, **404**, 59-61; (c) Q. Song and Z. J. Zhang, *J. Am. Chem. Soc.*, 2004, **126**, 6164-6168.
6. (a) H. G. Yang, C. H. Sun, S. Z. Qiao, J. Zou, G. Liu, S. C. Smith, H. M. Cheng and G. Q. Lu, *Nature*, 2008, **453**, 638-641; (b) Y. Dai, C. M. Cobley, J. Zeng, Y. Sun and Y. Xia, *Nano Lett.*, 2009, **9**, 2455-2459.
7. P. Joshi and M. Cole, *J. Appl. Phys.*, 1999, **86**, 871-880.
8. R. Bassiri, K. B. Borisenko, D. J. H. Cockayne, J. Hough, I. MacLaren and S. Rowan, *Appl. Phys. Lett.*, 2011, **98**.
9. J. Y. Duan, W. D. Shi, L. L. Xu, G. Y. Mou, Q. L. Xin and J. G. Guan, *Chem. Commun.*, 2012, **48**, 7301-7303.
10. (a) Y. N. Wu, L. Li and H. P. Cheng, *Phys. Rev. B*, 2011, **83**, 144105; (b) S. H. Lee, J. Kim, S. J. Kim, S. Kim and G. S. Park, *Phys. Rev. Lett.*, 2013, **110**, 235502; (c) B. R. Sahu and L. Kleinman, *Phys. Rev. B*, 2004, **69**, 165202; (d) X. J. Lu, Q. Y. Hu, W. G. Yang, L. G. Bai, H. Sheng, L. Wang, F. Q. Huang, J. G. Wen, D. J. Miller and Y. S. Zhao, *J. Am. Chem. Soc.*, 2013, **135**, 13947-13953.
11. Z. Wang, J. G. Hou, C. Yang, S. Q. Jiao, K. Huang and H. M. Zhu, *Energy Environ. Sci.*, 2013, **6**, 2134-2144.
12. (a) E. Barsoukov and J. R. Macdonald, *Impedance spectroscopy: theory, experiment, and applications*, John Wiley & Sons, 2005; (b) S. P. S. Badwal, *J. Mater. Sci.*, 1984, **19**, 1767-1776.
13. H. Cheng, B. Huang and Y. Dai, *Nanoscale*, 2014, **6**, 2009-2026.
14. S. F. Ho, S. Contarini and J. W. Rabalais, *J. Phys. Chem.*, 1987, **91**, 4779-4788.
15. (a) T. Grzybowski, *High Pressure in Science and Technology. III.--General Topics*, 1983, 43-47; (b) M. Cetinkol, A. P. Wilkinson, C. Lind, W. A. Bassett and C.-S. Zha, *J. Phys. Chem. Solids*, 2007, **68**, 611-616.
16. C. R. Morelock, B. K. Greve, M. Cetinkol, K. W. Chapman, P. J. Chupas and A. P. Wilkinson, *Chem. Mater.*, 2013, **25**, 1900-1904.
17. L. Onsager, *Phys. Rev.*, 1944, **65**, 117-149.
18. R. L. Penn and J. F. Banfield, *Science*, 1998, **281**, 969-971.
19. M. Siodmiak, G. Frenking and A. Korkin, *J. Phys. Chem. A*, 2000, **104**, 1186-1195.
20. P. Čapková and J. Walter, *J. Solid State Chem.*, 2000, **149**, 68-74.
21. Z. L. Wang, *J. Phys. Chem. B*, 2000, **104**, 1153-1175.
22. (a) X. a. Fan, J. Guan, Z. Li, F. Mou, G. Tong and W. Wang, *J. Mater. Chem.*, 2010, **20**, 1676-1682; (b) Y. Sun and Y. Xia, *Science*, 2002, **298**, 2176-2179.
23. (a) A. C. Shi and M. Wortis, *Phys. Rev. B*, 1988, **37**, 7793-7805; (b) P. Geysermans, F. Finocchi, J. Goniakowski, R. Hacquart and J. Jupille, *Phys. Chem. Chem. Phys.*, 2009, **11**, 2228-2233; (c) X. C. Ma, Y. Dai, J. B. Lu, M. Guo and B. B. Huang, *J. Phys. Chem. C*, 2012, **116**, 19372-19378.